Efficient Two-Band based Non-Equilibrium Green's Function Scheme for Modeling Tunneling Nano-Devices

Hamilton Carrillo-Nuñez[1], Jaehyun Lee[1], Salim Berrada[1], Cristina Medina-Bailón[1], Mathieu Luisier[2], Asen Asenov[1], and Vihar P. Georgiev[1]
[1]University of Glasgow, School of Engineering, Rankine Building, Oakfield Avenue, Glasgow, G12 8LT
[2]Integrated Systems Laboratory ETH Zürich, Gloriastrasse 35, 8092, Zürich, Switzerland

***Abstract*—In this work, we introduce a novel procedure to compute the direct band-to-band tunneling in semiconductor nano-devices by combining the effective mass approximation, the non-equilibrium Greens function technique, and the two-band Flietner model of the imaginary dispersion. The model is first tested on a Si-InAs nanowire p-type tunnel field-effect transistor (p-TFET), showing great accuracy at much less computational cost when compared with atomistic simulations. Secondly, we report a preliminary quantum transport simulation study of the impact of random discrete dopants on Si-InAs nanowire p-TFETs. An ensemble of 63 InAs-Si nanowire TFETs has been simulated, revealing a strong dopant-induced variability.**

I. Introduction

Over the last decade, the interest in band-to-band tunneling (BTBT) devices has dramatically increased due to their sharp switching characteristics, which makes them potential candidates for low-power electronic applications [1]. The most popular BTBT devices are the Tunneling Field-Effect Transistors (TFETs) that, in theory, could achieve sub-thermal subthreshold swing (SS), i.e. $SS < 60$ mV/decade.

At the nanometer scale and in the presence of tunneling, quantum transport simulations are required to accurately describe TFET operation and predict its performance. Few analytical models exist in the literature to compute the BTBT accounting for quantum effects, such as geometrical confinement. These are mostly based on the one-band model of the imaginary dispersion [2], [3]. Also there are two- band models, such as Kane [4] or Flietner [5] model, which are commonly implemented in semiclassical tools based on the Wentzel, Kramers, and Brillouin (WKB) approximation [6], [7].

In this work, the coupled mode-space non-equilibrium Greens function (NEGF) scheme within the effective mass approximation (EMA), and the Flietner model of the imaginary dispersion are implemented into a novel procedure to compute the direct BTBT in nano-devices. For benchmarking, the simulations of a Si-InAs nanowire p-TFET are compared with those from the atomistic OMEN tool [8].

The paper is organized as follows. The BTBT model and simulation methodology is presented in Section II. Then, the comparison with atomistic simulations and main findings from the statistical analysis are presented in Section III. Finally, the conclusions are drawn in Section IV.

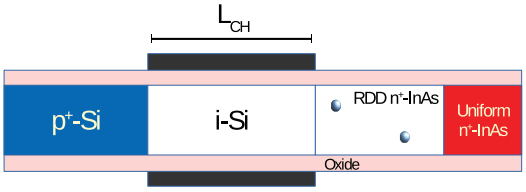

Fig. 1. Sketch of the Si-InAs nanowire TFET along the transport direction considered in this work. The gate is 15 nm long and is all-around the intrinsic Si region. As the tunneling is mainly happening at the InAs and i-Si interface, RDD is only considered in the InAs region. The nanowire diameter is 3.5 nm and the effective oxide thickness is 0.46 nm.

II. BTBT model and Simulation Methodology

The valence and conduction band edges are connected by using the two-band model of the imaginary dispersion proposed by Flietner in Ref. [5]. For quantum transport simulations, the Flietner model can be rewritten as [3]:

$$\frac{\hbar^2 k^2}{2m_0} = \frac{E_{\rm g}(E-E_{\rm c})(E-E_{\rm v})}{\left[\sqrt{\frac{m_0}{m_{\rm c}}}(E-E_{\rm c}) - \sqrt{\frac{m_0}{m_{\rm v}}}(E-E_{\rm v})\right]^2}, \quad (1)$$

where $E_{\rm g}$ and $m_{\rm c(v)}$ are the band gap energy and the conduction (valence) effective mass, respectively. The rest of the parameters takes their usual meaning. Contrary to the Kane model, both the real conduction and valence bands in the vicinity of their extrema are correctly reproduced,

$$E \approx E_{\rm c(v)} \pm \frac{\hbar^2 k^2}{2m_{\rm c(v)}} + \cdots . \quad (2)$$

Here, $E_{\rm c(v)}$ is the conduction (valence) band edge. This is advantageous since by including an external potential $U(\mathbf{r})$ in Eq. (2)

$$E \approx E_{\rm c(v)} + U(\mathbf{r}) \pm \frac{\hbar^2 k^2}{2m_{\rm c(v)}} + \cdots . \quad (3)$$

One can set up the appropriate envelope equation for low-dimensional semiconductors that incorporates both real and imaginary branches of the total band structure.

978-1-5386-6790-3/18/$31.00 ©2018 IEEE

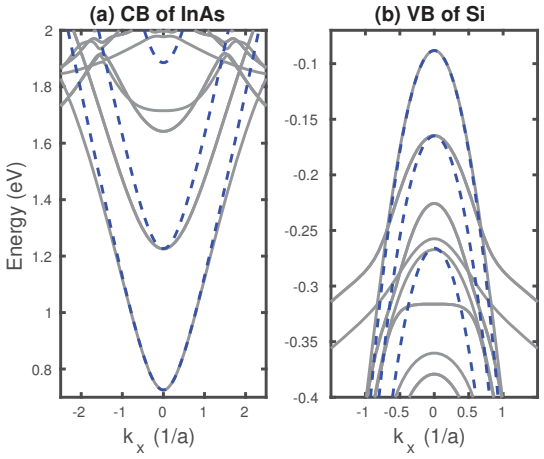

Fig. 2. Comparison of the conduction (CB) and valence (VB) full-band structure with their corresponding fitted effective mass (EMA) band structure of (a) InAs and (b) Si, respectively. The crystalographic direction is $\langle 111 \rangle$. The full-band structures have been computed with the atomistic OMEN tool. In case of the EMA-CB of InAs, band non-parabolicity corrections are included.

Following, the quantum transport problem for electrons and holes is independently solved within the EMA, by using the NEGF technique in mode-space representation and coupled self consistently to the Poisson equation. The total carrier density determines the new potential. Once the convergence is reached, the valence and conduction bands are bridged through the two-band model of the imaginary dispersion proposed by Flietner and the BTBT current is computed by solving the following envelope equation,

$$-\frac{\hbar^2}{2m_0}\frac{\partial^2\chi}{\partial x^2} = \frac{E_{\rm g}(E-U_{\rm c})(E-U_{\rm v})}{\left[\sqrt{\frac{m_0}{m_{\rm c}}}(E-U_{\rm c}) - \sqrt{\frac{m_0}{m_{\rm v}}}(E-U_{\rm v})\right]^2}\chi = F(E,U_{\rm c},U_{\rm v})\chi, \quad (4)$$

with open boundary conditions. In the latter, $U_{\rm c(v)}$ corresponds to the lowest conduction (highest valence) subband energy, and the coordinate x has been omitted for brevity. Finally, by defining a two-band Hamiltonian as

$$H = -\frac{\hbar^2}{2m_0}\frac{\partial^2}{\partial x^2} - F(E,U_{\rm c},U_{\rm v}) + E, \quad (5)$$

Eq. (4) can be solved to calculate the BTBT current in nanowire tunneling devices by means of a NEGF scheme.

III. Results and Discussion

Fig. 1 shows the sketch of a Si-InAs nanowire TFET considered in this work. The gate is 15 nm long, covering all-around the intrinsic Si nanowire region, and the nanowire diameter is $2R = 3.5$ nm. The transport occurs along the $\langle 111 \rangle$ crystallography direction. The p^+-type (Si) drain and n^+-type (InAs) source are highly doped with $N_{\rm A} = 2\times10^{20}{\rm cm}^{-3}$ and $N_{\rm D} = 10^{19}{\rm cm}^{-3}$, respectively. The effective oxide thickness is 0.46 nm and the applied source-to-drain bias ($V_{\rm DS}$) is fixed to -1.0 V. The devices are simulated at room temperature.

The electron and hole effective masses are extracted from the full-band structure computed with the atomistic tool OMEN [8], based on the $sp^3d^5s^*$ tight-binding model. For the InAs nanowire the masses are $m_{\rm c} = (0.072m_0,\ 0.22m_0,\ 0.22m_0)$ and $m_{\rm v} = (0.072m_0,\ 0.26m_0,\ 0.26m_0)$. In case of Si, $m_{\rm c} = (0.45m_0, 0.27m_0, 0.27m_0)$ and $m_{\rm v} = (0.11m_0, 1.44m_0, 1.44m_0)$. The full-band structure of the InAs and Si nanowires are plotted in Fig. 2(a) and Fig. 2(b), respectively. Both were computed with the atomistic tool OMEN. The dashed-blue lines are the fitted parabolic band structure. Notice that in the case of the InAs the band non-parabolicity corrections are also taken into account.

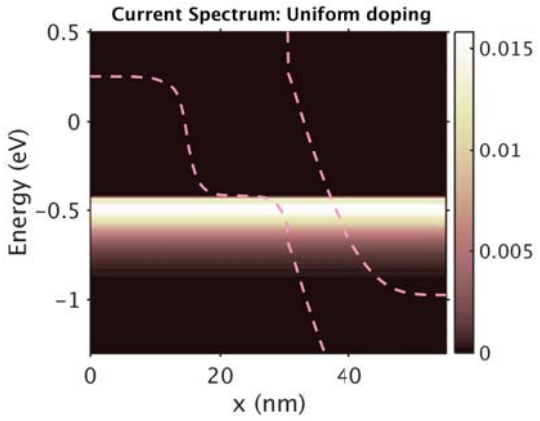

Fig. 3. Simulated ON-state current-spectra of the Si-InAs nanowire TFET, in Fig. 1, with uniform doping concentrations. The pink dashed-lines denote the highest valence and lowest conduction subbands. Notice that the BTBT is mainly happening between the i-Si and InAs regions.

First, we have simulated a Si-InAs nanowire TFET with uniform doping at source and drain. Fig. 3 shows the ON-state current spectrum computed with the EMA-Flietner based NEGF scheme introduced here. As observed, the shorter the tunneling path, the highest the current spectrum. Moreover, the BTBT mainly happens between the i-Si and InAs. The latter is agreement with the results reported in Ref. [7].

Fig. 4 shows the comparison of the $I_{\rm D} - V_{\rm GS}$ characteristic computed with EMA-Flietner based NEGF scheme, and the

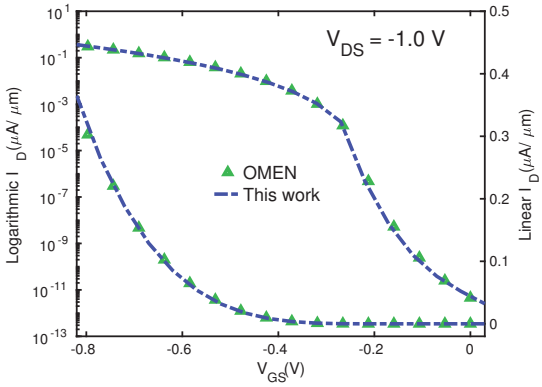

Fig. 4. The EMA-Flietner NEGF vs. OMEN $I_{\rm D} - V_{\rm GS}$ characteristics of the Si-InAs nanowire TFET shown in Fig. 1. For this comparison, the InAs region was assumed to be uniformly doped and the current was normalized by $2\pi R$. The $I_{\rm D} - V_{\rm GS}$ characteristics computed with OMEN was taken from Ref. [7].

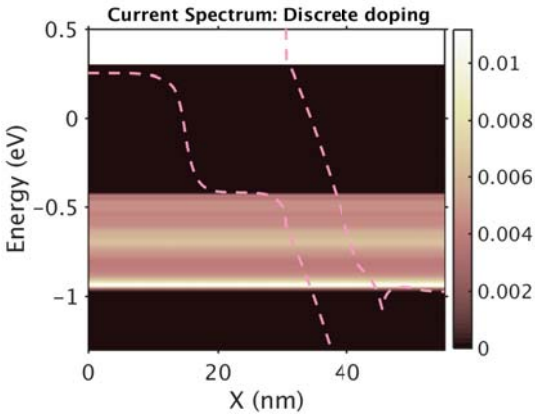

Fig. 5. Simulated ON-state current-spectra of the Si-InAs nanowire TFET, in Fig. 1, with two random distributed dopants located at $x = 41$ nm and $x = 45$ nm. Notice how the discrete dopants highly impact the potential and subband profiles. In this particular configuration, their position enhance the ON-current. The pink dashed-lines denote the highest valence and lowest conduction subbands.

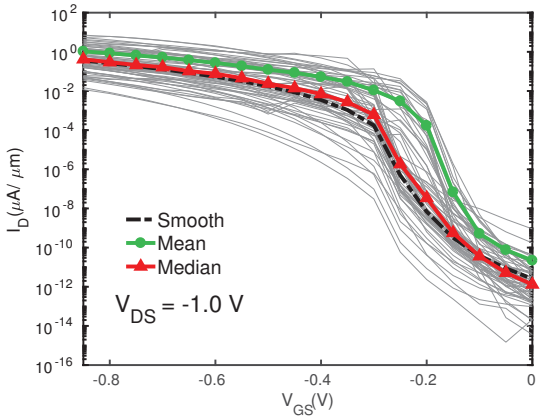

Fig. 6. $I_{\rm D} - V_{\rm GS}$ characteristics of an ensemble of 63 Si-InAs nanowire TFETs with random distributed dopants (gray curves). For this study and just to show the strong variability due to RDD, the number of dopants is fixed to 2. The statistical mean and median are also plotted. The Si-InAs nanowire TFET with uniform doping profile is shown as reference. The median and uniform curves are in good agreement, whereas the mean curve is biased to the higher curves. The current was normalized by $2\pi R$. As one can see the impact

one obtained with OMEN, reported in Ref. [7]. Note that the agreement is excellent. This result is very important for future predictions and studies of Si-InAs nanowire TFETs, such as the impact of random distributed dopants (RDDs). For the latter, tens of simulations are needed for a proper statistical analysis. The scheme proposed in this work offers a very efficient alternative to atomistic simulations. It allows the simulations of hundreds of nanowire TFETs at much less computational cost with atomistic accuracy.

Fig. 5 illustrates the impact of randomly located dopants on the ON-state current spectrum with dopants located at $x = 41$ nm and $x = 45$ nm. Notice how the discrete dopants highly impact the potential and subband profiles. In this particular configuration, their position favors the ON-state current. The RDD region is only considered in the InAs part of the device,

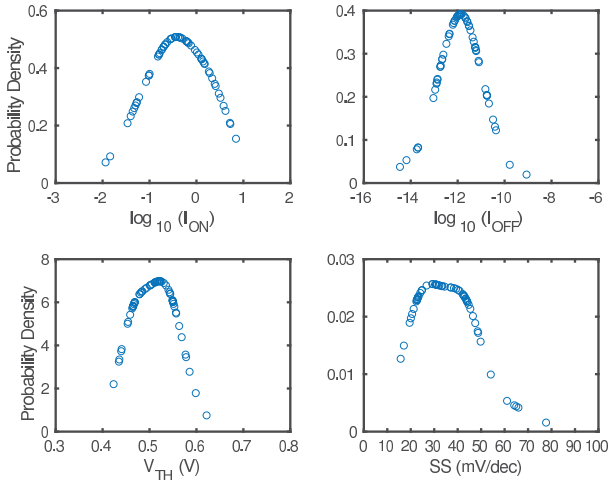

Fig. 7. Probability density functions of the most important Figures of Merit obtained from the simulation of the ensemble of the 63 Si-InAs nanowrie TFETs shown in Fig. 6.

being 20 nm long. The number of dopants in each of the TFETs is fixed to 2, which is the number of dopants that can exist in the RDD volume.

For a suitable statistical analysis an ensemble of 63 Si-InAs nanowire TFETs with RDD have been simulated. Their corresponding $I_{\rm D} - V_{\rm GS}$ characteristics are shown in Fig. 6. Observe the strong impact of RDD on the BTBT current over the entire gate voltage range. The mean, median, and smooth curves are also included for comparison. The smooth curve correspond to the device with uniform doping at source and drain regions. As expected, the median and smooth $I_{\rm D} - V_{\rm GS}$ characteristics are in very good agreement. Whereas, the mean and median $I_{\rm D} - V_{\rm GS}$ characteristics differs from each other, especially at high gate voltage. Their corresponding ON-state currents are also different. Contrary to MOSFETs, we find that the ON-state currents of TFETs with RDD-induced variability are described by a logarithmic-normal distribution (see Fig. 7 top-left), varying over three orders of magnitude. This can be understood by keeping in mind that the ON-state in a TFET is still controlled by the BTBT barrier length. In the presence of RDDs, the barrier width and height, as well as the Figures of Merit (FoM), depends on the number of dopants and their position.

Fig. 7 shows the probability distribution functions (PDFs) of the most relevant FoM: $\log_{10}(I_{\rm ON})$, $\log_{10}(I_{\rm OFF})$, $\rm V_{TH}$, and SS. The latter is computed as $SS = \sum_j SS(V_{{\rm GS},j})\Delta V_{{\rm GS},j} / \sum_j \Delta V_{{\rm GS},j}$, within a range of $\sum_j \Delta V_{{\rm GS},j} = 250$ mV, starting at $V_{\rm GS,0} = V_{\rm GS} = 0$ V. A logarithmic distribution for the ON- and OFF-currents has been used to calculate their PDFs. The OFF- and ON-state currents varies over six and three orders of magnitude, respectively. As seen in Fig. 7, the PDFs reveals a variation of 0.2 V in the $\rm V_{TH}$, whereas in case of the SS the RDD impact is much more pronounced. The SS varies approximately from 20 mV/decade to 80 mV/decade.

Finally, we would like to point out that for a more accurate

study, the number of dopants in each of the TFETs should be randomly chosen from a Poisson distribution, placing them by means of a probability rejection technique. The mean is determined by the doping concentration multiplied by the volume of the RDD region. However, it would also required a much larger ensemble of simulated devices. This is out of the scope of this work and would be addressed elsewhere.

IV. Conclusion

We have developed and implemented a new efficient two-band based NEGF procedure to compute the BTBT in nano-devices. In this work, we just considered the case of InAs-Si nanowire TFETs with uniform doping and random distributed dopants. For the former, a direct comparison with atomistic results showed an excellent agreement. For the latter, an ensemble of 63 InAs-Si nanowire TFETs has been simulated, revealing that RDDs might have a strong dopant-induced variability on TFETs.

V. Acknowledgment

This work was supported by the U.K. EPSRC (Projecst No. EP/P009972/1 and No. EP/S001131/1).

References

[1] A. M. Ionescu and H. Riel, "Tunnel field-effect transistors as energy-efficient electronic switches," *Nature*, vol. 479, pp. 329–337, 2011.

[2] W. G. Vandenberghe, B. Sore, W. Magnus, G. Groeseneken, and M. V. Fischetti, "Impact of field-induced quantum confinement in tunneling field-effect devices," *Applied Physics Letters*, vol. 98, no. 14, p. 143503, 2011. [Online]. Available: https://doi.org/10.1063/1.3573812

[3] H. Carrillo-Nuñez, A. Ziegler, M. Luisier, and A. Schenk, "Modeling direct band-to-band tunneling: From bulk to quantum-confined semiconductor devices," *Journal of Applied Physics*, vol. 117, no. 23, p. 234501, 2015. [Online]. Available: https://doi.org/10.1063/1.4922427

[4] E. O. Kane, "Zener tunneling in semiconductors," *J. Phys. and Chem. of Solids*, vol. 12, pp. 181–188, 1960.

[5] H. Flietner, "The E(k) relation for a 2-band scheme of semiconductors and the application to metal-semiconductor contact," *Phys. Stat. Sol. (b)*, vol. 54, pp. 201–208, 1972.

[6] *Sentaurus-Device User Guide*, 09th ed., Synopsys Inc., Mountain View, California, 2013.

[7] H. Carrillo-Nuñez, M. Luisier, and A. Schenk, "Analysis of InAs-Si heterojunction nanowire tunnel FETs: extreme confinement vs. bulk," *Solid-state Elect.*, vol. 113, pp. 61–63, 2015.

[8] M. Luisier, A. Schenk, W. Fichtner, and G. Klimeck, "Atomistic simulation of nanowires in the $sp^3d^5s^*$ tight-binding formalism: From boundary conditions to strain calculations," *Phys. Rev. B*, vol. 73, p. 165319, 2006.